

Provided for non-commercial research and education use.  
Not for reproduction, distribution or commercial use.



This article appeared in a journal published by Elsevier. The attached copy is furnished to the author for internal non-commercial research and education use, including for instruction at the authors institution and sharing with colleagues.

Other uses, including reproduction and distribution, or selling or licensing copies, or posting to personal, institutional or third party websites are prohibited.

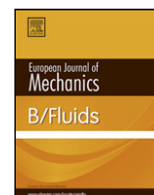
In most cases authors are permitted to post their version of the article (e.g. in Word or Tex form) to their personal website or institutional repository. Authors requiring further information regarding Elsevier's archiving and manuscript policies are encouraged to visit:

<http://www.elsevier.com/copyright>



Contents lists available at ScienceDirect

## European Journal of Mechanics B/Fluids

journal homepage: [www.elsevier.com/locate/ejmflu](http://www.elsevier.com/locate/ejmflu)

# The influence of thermal relaxation on the oscillatory properties of two-gradient convection in a vertical slot

N.C. Papanicolaou<sup>a</sup>, C.I. Christov<sup>b</sup>, P.M. Jordan<sup>c,\*</sup>

<sup>a</sup> Department of Computer Science, University of Nicosia, P.O. Box 24005, 1700 Nicosia, Cyprus

<sup>b</sup> Department of Mathematics, University of Louisiana at Lafayette, Lafayette, LA 70504, USA

<sup>c</sup> Code 7181, Naval Research Laboratory, Stennis Space Center, MS 39529, USA

## ARTICLE INFO

### Article history:

Received 30 April 2010

Received in revised form

10 September 2010

Accepted 14 September 2010

Available online 22 September 2010

### Keywords:

Maxwell–Cattaneo law

Two-gradient convection

Beam functions

Straughan number

## ABSTRACT

We study the effects of the Maxwell–Cattaneo (MC) law of heat conduction on the flow of a Newtonian fluid in a vertical slot subject to both vertical and horizontal temperature gradients. Working in one spatial dimension (1D), we employ a spectral expansion involving Rayleigh's beam functions as the basis set, which are especially well-suited to the fourth order boundary value problem (b.v.p.) considered here, and the stability of the resulting dynamical system for the Galerkin coefficients is investigated. It is shown that the absolute value of the (negative) real parts of the eigenvalues are reduced, while the absolute values of the imaginary parts are somewhat increased, under the MC law. This means that the presence of the time derivative of the heat flux increases the order of the system, thus leading to more oscillatory regimes in comparison with the usual Fourier case. Moreover, no eigenvalues with positive real parts were found, which means that in this particular situation, the inclusion of thermal relaxation does not lead to destabilization of the motion.

Published by Elsevier Masson SAS.

## 1. Introduction

One of the main shortcomings of Fourier's law of heat conduction is that it leads to a parabolic equation for the temperature field. This means that any initial disturbance is felt instantly, but unequally, throughout the entire medium in question. This behavior is said to contradict the principle of causality; and is known as the 'paradox of heat conduction'. To remedy this unrealistic feature, various modifications of Fourier's law have been proposed over the years, not all of which have been successful (see, e.g., [1]). Of the formulations that have proven physically acceptable, the best known is the Maxwell–Cattaneo (MC) law of heat conduction [2–6], which on denoting the thermal conductivity as  $K(>0)$  assumes the form

$$(1 + \tau_0 \partial_t) \mathbf{q} = -K \nabla T. \quad (1)$$

Here,  $T$  denotes the absolute temperature;  $\mathbf{q}$  is the heat flux vector;  $\partial_t$  stands for  $\partial/\partial t$ ; the thermal relaxation time  $\tau_0(>0)$ , which along with  $K$  is hereafter taken to be constant, represents the time lag required to establish steady heat conduction in a volume element once a temperature gradient has been imposed across it [4]; and it should be noted that the MC law reduces to Fourier's law when  $\tau_0 := 0$ .

We observe that the time rate appearing in the MC law is merely a partial time derivative. As a result,  $\mathbf{q}$  can be eliminated between Eq. (1) and the energy balance law

$$\rho c_p (\partial_t T + \mathbf{v} \cdot \nabla T) = -\nabla \cdot \mathbf{q}, \quad (2)$$

where  $\mathbf{v}$  is the velocity vector and it is assumed that no thermal sources/sinks are present, to arrive at the following equation for the temperature field:

$$\tau_0 [T_{tt} + (\mathbf{v} \cdot \nabla T)_t] + T_t + \mathbf{v} \cdot \nabla T = \tau_0 c^2 \nabla^2 T, \quad (3)$$

where  $\kappa = K/(\rho c_p)$  is the thermal diffusivity and  $c = \sqrt{\kappa/\tau_0}$ . In the case of a continuum at rest, Eq. (3) reduces to the damped wave equation, which is hyperbolic. Thus, when  $\mathbf{v} = \mathbf{0}$ , Eq. (3) predicts that heat conduction occurs via the propagation of damped thermal waves of finite speed  $c$ , a phenomenon known as 'second sound' [2,3].

In order to understand the role played by the time derivative in the MC law, one needs to consider flow problems that involve sufficiently rich phenomenology, but with extremely simple geometry. The problem of 2D convection in a horizontal layer considered in [6–8] provides a situation in which the additional terms could influence the solution, but the physics contained therein may be obscured by the mathematical complications associated with the finite, 2D geometry. Clearly, a 1D flow offers the needed simplicity for separating out these different effects. However, in 1D convective flow (regardless of whether it is in a horizontal or vertical

\* Corresponding author.

E-mail address: [pjordan@nrlssc.navy.mil](mailto:pjordan@nrlssc.navy.mil) (P.M. Jordan).

layer with differentially heated walls), the convective terms cancel identically if the temperature has only one (horizontal or vertical) gradient.

For this reason, in this article, we turn our attention to the problem of convective flow in a vertical slot, first considered in [9], in which the temperatures of the walls are not merely different, but are also functions of the vertical coordinate. This flow was found to exhibit a rich phenomenology, especially in the case of modulations of the gravitational acceleration: The so-called ‘g-jitter’ effect. The latter was studied by Homsy and co-workers and interesting routes to parametric instability were uncovered; see [10–16]. In what follows, we shall refer to this type of flow as ‘two-gradient convection’. It seems that even without the g-jitter effect, this flow configuration can be a good testing ground in which to study the effect that the MC law has on free convection.

## 2. Convection in a vertical slot

Consider now an infinite vertical slot, of width  $2h$ , filled with a thermally conducting Newtonian fluid. Taking the  $x$ - and  $y$ -axes of a Cartesian coordinate system perpendicular and parallel to, respectively, the axis of the slot, we place the left and right walls of the slot at  $x = -h$  and  $x = h$ , respectively. (For the details of the geometry and the flow configuration, we refer the reader to [14,16]).

For incompressible convective flows, the current approach involves the use of what has come to be known as the Boussinesq approximation, wherein the dependence of density on pressure is neglected. Assuming, as usual, that the fluid’s coefficient of thermal expansion,  $\alpha$ , is very small, the Boussinesq-based model reads

$$\frac{\partial \mathbf{v}}{\partial t} + \mathbf{v} \cdot \nabla \mathbf{v} = -\alpha g(T - T_R)\mathbf{j} + \nu \Delta \mathbf{v}, \quad (4)$$

where hereafter the velocity vector assumes the form  $\mathbf{v} = (u, v)$ ,  $\nu$  is the kinematic viscosity,  $g$  is the acceleration due to gravity, and  $\mathbf{j}$  is a unit vector in the vertical direction. In addition,  $T_R$  is some reference value of the temperature and the difference  $T - T_R$  is also assumed to be small, so that quadratic and higher terms can be neglected in the expansion relating the density to the temperature, as the Boussinesq approximation allows. Thus, Eqs. (3) and (4) form a closed system for the unknowns  $\mathbf{v}$ ,  $T$ .

Let us define the reference temperature as  $T_R = (T_+ + T_-)/2$ , where  $T_-$  and  $T_+$  are the temperatures of the left and right walls at vertical position  $y = 0$ . Then  $\beta = (T_+ - T_-)/h$  denotes the horizontal temperature difference, where  $T_+ > T_-$  is assumed. In addition,  $\Delta_T$  denotes the imposed vertical gradient of the wall temperature (a constant). Letting  $\delta = \Delta_T/\beta$ , we define the dimensionless perturbations of temperature  $\theta$  and heat flux  $\hat{\mathbf{q}}$  as follows:

$$T - T_R = \left( \theta + \frac{1}{2} \frac{x}{h} + \delta \frac{y}{h} \right) h\beta, \quad \mathbf{q} = (\hat{\mathbf{q}} + \delta \mathbf{j})\beta K. \quad (5)$$

Now, since the flow is not created by a prescribed velocity at the boundary, it is convenient to set  $U = \nu/h$  as the velocity scale and to introduce the following dimensionless variables:

$$t = \hat{t} \frac{h}{U} = \hat{t} \frac{h^2}{\nu}, \quad x = h\hat{x}, \quad (6)$$

$$y = h\hat{y}, \quad u = \hat{u}U, \quad v = \hat{v}U,$$

along with the dimensionless constants

$$\text{Sg} = \frac{\tau_0 \nu}{h^2}, \quad \text{Ra} = \frac{g\alpha \Delta_T h^4}{\nu^2}, \quad \text{Pr} = \frac{\nu}{\kappa}, \quad (7)$$

which are termed the Straughan,<sup>1</sup> Rayleigh, and Prandtl numbers

<sup>1</sup> What we refer to as the Straughan number, Sg, is named here in honor of Prof. Brian Straughan, whose pioneering work on the impact of thermal inertia on convection has been the inspiration for the present paper.

respectively. After the derivation of the dimensionless system, the hats can be omitted without fear of confusion. It should be noted that  $\text{Sg} = \tau_c \text{Pr}$ , where  $\tau_c = \frac{\tau_0 \kappa}{h^2}$  is known as the Cattaneo number [6]. In our view, as it involves the kinematic viscosity, the Straughan number is the more pertinent parameter when considering thermal convection in viscous fluids; indeed, the Straughan number is directly connected with the effects of thermal inertia: A large Sg implies a large thermal inertia, while  $\text{Sg} := 0$  gives Fourier’s law.

The posing of the present problem has been sketched-out in [17], where it was shown that the only nontrivial velocity component is the vertical one, i.e.,  $v$ , and that the first momentum equation reduces to  $\partial p/\partial x = 0$ . It can be shown that, in terms of the stream function  $\Psi$  (see [14,16] and the literature cited therein), the 1D equations of motion read

$$\frac{\partial^3 \Psi}{\partial x^2 \partial t} = -\frac{\text{Ra}}{\delta} \left[ \frac{\partial \theta(x, t)}{\partial x} + \frac{1}{2} \right] + \frac{\partial^4 \Psi}{\partial x^4}, \quad (8a)$$

$$\text{Sg} \left[ \frac{\partial^2 \theta}{\partial t^2} - \delta \frac{\partial^2 \Psi}{\partial x \partial t} \right] + \frac{\partial \theta}{\partial t} - \delta \frac{\partial \Psi}{\partial x} = \frac{1}{\text{Pr}} \frac{\partial^2 \theta}{\partial x^2}. \quad (8b)$$

The dimensionless boundary conditions (b.c.’s) read

$$\Psi(\pm 1, t) = \partial_x \Psi|_{x=\pm 1} = 0, \quad \theta(\pm 1, t) = 0, \quad (9)$$

which express the non-slip conditions and the fact that  $\theta$  is the perturbation of the main linear temperature profile.

## 3. Formulation as a single equation

First, we eliminate the temperature from Eqs. (8) by differentiating Eq. (8b) with respect to  $x$  and then introduce  $\theta_x$  from Eq. (8a) to obtain

$$\begin{aligned} & \text{Sg}(\Psi_{t^2 x^4} - \Psi_{t^3 x^2} - \text{Ra}\Psi_{txx}) - \text{Ra}\Psi_{xx} + \Psi_{tx^4} - \Psi_{t^2 x^2} \\ & = \frac{1}{\text{Pr}}[-\Psi_{tx^4} + \Psi_{x^6}], \quad \psi_{t^k x^n} \stackrel{\text{def}}{=} \frac{\partial^{k+n} \psi}{\partial t^k \partial x^n}. \end{aligned} \quad (10)$$

Note that in this formulation, the parameter  $\delta$  serendipitously cancels. This does not mean that  $\delta$  has no role to play as an independent parameter; indeed, it provides the scale for the temperature field, which emerges after the integration of the above equation for the stream function. (Actually, in 2D such a reduction is not possible.)

Here, we note the interesting limit  $\text{Sg} \rightarrow \infty$ , which reduces Eq. (10) to the following single equation for the stream function:

$$\Psi_{t^2 x^4} - \Psi_{t^3 x^2} - \text{Ra}\Psi_{txx} = 0. \quad (11)$$

This equation can thus provide a check of the results for the full system for very large values of Sg. However, it must be understood that Eq. (11) does not correspond to the type II model of Green–Naghdi, which arises when the limit  $\tau_0 \rightarrow 0$  is taken under the assumption  $K \propto \tau_0$ ; see, e.g., Ref. [18] and those therein.

## 4. Estimates

We begin this section by using the boundary conditions for  $\Psi$  to evaluate the following integrals:

$$\int_{-1}^1 \Psi_t \Psi_{x^6} dx = -\frac{1}{2} \frac{d}{dt} \int_{-1}^1 (\Psi_{x^3})^2 dx, \quad (12a)$$

$$\int_{-1}^1 \Psi_t \Psi_{xx} dx = -\frac{1}{2} \frac{d}{dt} \int_{-1}^1 (\Psi_x)^2 dx, \quad (12b)$$

$$\int_{-1}^1 \Psi_t \Psi_{t^2 x^4} dx = \frac{1}{2} \frac{d}{dt} \int_{-1}^1 (\Psi_{txx})^2 dx, \quad (12c)$$

$$\int_{-1}^1 \psi_t \psi_{t^2 x^2} dx = -\frac{1}{2} \frac{d}{dt} \int_{-1}^1 (\psi_{tx})^2 dx, \quad (12d)$$

$$\int_{-1}^1 \psi_t \psi_{tx^4} dx = \int_{-1}^1 (\psi_{tx^2})^2 dx, \quad (12e)$$

$$\int_{-1}^1 \psi_t \psi_{tx^2} dx = -\int_{-1}^1 (\psi_{tx})^2 dx, \quad (12f)$$

$$\int_{-1}^1 [\psi_t \psi_{t^3 x^2} + (\psi_{t^2 x})^2] dx = -\frac{1}{2} \frac{d^2}{dt^2} \int_{-1}^1 (\psi_{tx})^2 dx. \quad (12g)$$

Note that  $\psi_x|_{x=\pm 1} = 0$  yields  $\psi_{tx}|_{x=\pm 1} = 0$ . Also, the condition that  $\psi$  is an even function gives  $\psi_{txx}|_{x=1} = \psi_{txx}|_{x=-1}$ .

Multiplying Eq. (10) by  $\psi_t$  and integrating with respect to  $x$  from  $-1$  to  $1$ , we obtain

$$\frac{1}{2} \text{Sg} \frac{d^2}{dt^2} \int_{-1}^1 (\psi_{tx})^2 dx + \frac{dE}{dt} = -\mathcal{D}, \quad (13)$$

where the energy and dissipation functionals are given by

$$E \stackrel{\text{def}}{=} \frac{1}{2} \int_{-1}^1 \left[ \frac{1}{\text{Pr}} (\psi_{xxx})^2 + \text{Sg} (\psi_{txx})^2 + \text{Ra} (\psi_x)^2 + (\psi_{tx})^2 \right] dx, \quad (14a)$$

$$\mathcal{D} \stackrel{\text{def}}{=} \int_{-1}^1 \left[ \left(1 + \frac{1}{\text{Pr}}\right) (\psi_{txx})^2 + \text{SgRa} (\psi_{tx})^2 + \text{Sg} (\psi_{ttx})^2 \right] dx. \quad (14b)$$

Since  $\text{Sg} > 0$ , the qualitative behavior of the system is expected to be damped oscillatory, but stable. It should be noted here that the case for stability can be argued by using different embedding inequalities to bracket the first term in Eq. (13) by the energy functional, leading to a differential inequality for  $E$ . However, this goes beyond the scope of the present work. Note also that if  $\text{Sg} := 0$  is taken, the first term in Eq. (13), which contains the second time derivative of a positive-definite functional, is not present, which implies stability in the case of Fourier's law.

### 5. The steady convection

The above problem admits a stationary solution (i.e., the 'undisturbed state'), namely,  $\psi^*(x)$ ,  $\theta^*(x)$ , for which Eqs. (8) reduce to:

$$\frac{\text{Ra}}{\delta} \left[ \frac{d\theta^*}{dx} + \frac{1}{2} \right] + \frac{d^4 \psi^*}{dx^4} = 0, \quad (15a)$$

$$-\delta \frac{d\psi^*}{dx} = \frac{1}{\text{Pr}} \frac{d^2 \theta^*}{dx^2}. \quad (15b)$$

Let us now integrate Eq. (15a) and use the fact that  $\psi^*$  is an even function, while  $\theta^*$  is odd. Thus,

$$-\text{Ra} \left[ \theta^* + \frac{1}{2} x \right] + \delta \frac{d^3 \psi^*}{dx^3} = 0, \quad (16)$$

Then, we differentiate Eq. (15b) twice and introduce the result into Eq. (16), thus yielding

$$\frac{d^4 \theta^*}{dx^4} + \text{Ry} \theta^* = -\frac{1}{2} \text{Ry} x, \quad \text{Ry} := \frac{\text{Ra}}{\text{Pr}} = \frac{g \alpha \Delta_T h^4}{\kappa \nu}, \quad (17)$$

where  $\text{Ry}$  is a version of the Rayleigh number often used in models of free convection.

Eq. (17) is of a higher order and therefore requires additional boundary conditions. The latter stem from Eq. (15b) taken at the boundaries when the b.c.'s for the derivative of the stream function are acknowledged, namely,

$$\left. \frac{d^2 \theta^*}{dx^2} \right|_{x=\pm 1} = 0. \quad (18)$$

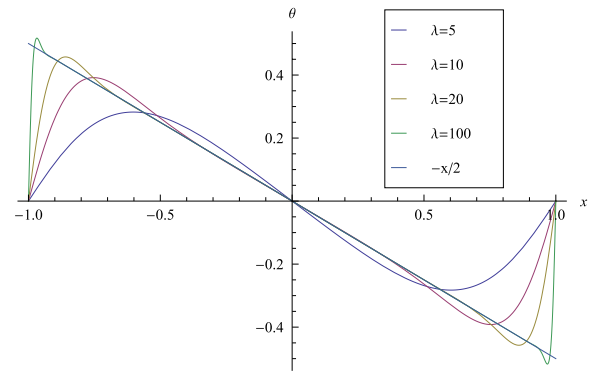


Fig. 1. Temperature distribution for different values of  $\lambda$ .

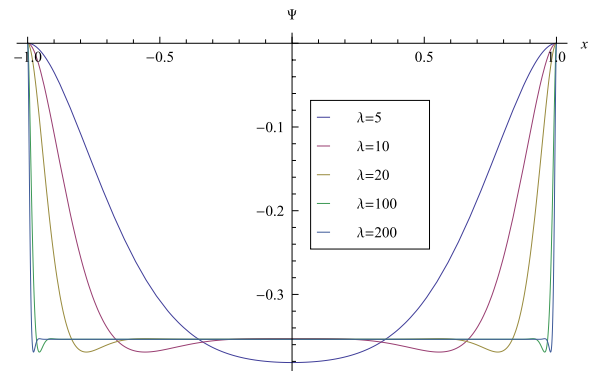


Fig. 2. Profile of the scaled stream function  $\psi_s$  for different  $\lambda$ .

The solution of Eq. (17) subject to the b.c.'s from Eqs. (9), (18) has the form

$$\begin{aligned} \theta^*(x) = & -\frac{1}{2} x - \frac{\cosh(\lambda) \cosh(\lambda x) \sin(\lambda) \sin(\lambda x)}{\cosh(\lambda) - \cos(\lambda)} \\ & + \frac{1}{2} \frac{\cos(\lambda) \cos(\lambda x) \sinh(\lambda) \sinh(\lambda x)}{\cosh(\lambda) - \cos(\lambda)}, \end{aligned} \quad (19a)$$

where  $\lambda = \sqrt[4]{\text{Ry}}/\sqrt{2}$ . The result for the temperature field is shown in Fig. 1. From the last equation one can easily determine that  $\psi^*$  is given by

$$\begin{aligned} \psi_s(x) := \frac{\delta}{\lambda} \text{Pr} \psi^*(x) = & -\frac{\cosh(\lambda) \cosh(\lambda x) \sin(\lambda) \cos(\lambda x)}{\cosh(2\lambda) - \cos(2\lambda)} \\ & - \frac{\cosh(\lambda) \sinh(\lambda x) \sin(\lambda) \sin(\lambda x)}{\sinh(2\lambda) - \cos(2\lambda)} \\ & + \frac{\cos(\lambda) \sin(\lambda x) \sinh(\lambda) \sinh(\lambda x)}{\cosh(2\lambda) - \cos(2\lambda)} \\ & - \frac{\cos(\lambda) \cos(\lambda x) \sinh(\lambda) \cosh(\lambda x)}{\cosh(2\lambda) - \cos(2\lambda)} \\ & - \frac{\sqrt{2} \sin(2\lambda) + \sinh(2\lambda)}{4 \cosh(2\lambda) - \cos(2\lambda)}, \end{aligned} \quad (19b)$$

where the 'scaled' stream function  $\psi_s$  is introduced for convenience of presentation. The profile of the stream function of the stationary solution is presented in Fig. 2

Clearly, boundary layers are formed near  $x = \pm 1$ , while in the core of the flow  $\theta^* \propto -\frac{1}{2} x$  and  $\psi^*$  is approximately constant. This can be easily verified if the independent variable is scaled by  $\lambda$  within the boundary layer. When this is done, as depicted in Fig. 3, we see that the four profiles are virtually indistinguishable, i.e., they present the solution inside the boundary layer, the latter not being affected by the flow in the core.

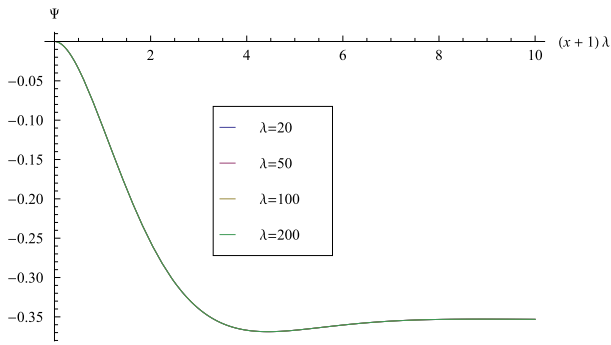


**Fig. 3.** Profile of the scaled stream function  $\psi_s$  as function of the scaled coordinate  $\xi = (x + 1)\lambda$  for different values of  $\lambda$ .

### 6. Beam–Galerkin expansion

Our approach to investigating the boundary value problems (8a), (8b), (9) is to use Galerkin expansions with Rayleigh beam functions [19] and harmonic functions as the basis sets, respectively. These functions satisfy the four b.c.'s for the stream function given in Eq. (9). Details of the application of the beam–Galerkin expansions can be found in [20,21]. Here, we follow [16], where the interaction with the harmonic functions is elaborated upon, and where all relevant formulas can be found.

Taking advantage of the symmetry, we expand the stream function  $\Psi$  into even Rayleigh beam functions and the temperature field,  $\Theta$ , into odd harmonic functions:

$$\Psi(x, t) = \sum_{i=1}^N p_i(t) c_i(x), \quad \Theta(x, t) = \sum_{i=1}^N d_i(t) \sin(i\pi x), \quad (20)$$

where  $N$  is sufficiently large to ensure an accurate approximation. As shown in the above cited works, the convergence of the series from Eq. (20) is fifth-order algebraic with  $N$ , thus making them very efficient.<sup>2</sup>

We substitute the above expansions into Eqs. (8), and employ the necessary expansion formulas (see the Appendix), to obtain the following dynamical system:

$$\sum_{j=1}^N \beta_{ij} \dot{p}_i = -\frac{\text{Ra}}{\delta} \sum_{i=1}^N i\pi \chi_{ij} d_i - \frac{\text{Ra}}{\delta} \frac{\sqrt{2} \tanh \kappa_j}{\kappa_j} + \kappa_j^4 p_j, \quad (21a)$$

$$\text{Sg} \ddot{d}_j - \text{Sg} \delta \sum_{i=1}^N b_{ij} \dot{p}_i + \dot{d}_j - \delta \sum_{i=1}^N b_{ij} p_i = -\frac{1}{\text{Pr}} j^2 \pi^2 d_j, \quad (21b)$$

where  $b_{ij} = \sum_{k=1}^N a_{ik} \hat{\sigma}_{kj}$ ,  $j = 1, 2, \dots, N$  (see the Appendix), and a superposed dot denotes a time derivative. For the sake of brevity, we introduce the following notation:

$$\begin{aligned} \mathbf{X} &:= \{i\pi \chi_{ij}\}, & \mathbf{B} &:= \{\beta_{ij}\}, & \mathbf{C} &= (\mathbf{B}^T)^{-1} := \{c_{ij}\}, \\ \mathbf{B} &:= \{b_{ij}\}, & \mathbf{h} &:= \{h_j\}, \\ \mathbf{K} &:= \{\kappa_j^4 \delta_{ij}\}, & \mathbf{\Pi}_2 &:= \{j^2 \pi^2 \delta_{ij}\}, \end{aligned} \quad (22)$$

along with the vectors

$$\mathbf{g}^a = -\frac{1}{2} \frac{\text{Ra}}{\delta} \mathbf{C} \mathbf{h}, \quad \mathbf{g}^b = \mathbf{0}, \quad \mathbf{g}^c = -\frac{1}{2} \text{Ra} \mathbf{B}^T \mathbf{C} \mathbf{h}.$$

It is convenient to introduce a new ‘composite’ vector of unknowns  $\mathbf{y}$  as follows:  $y_i := p_i$ ,  $y_{N+i} := d_i$ ,  $y_{2N+i} := \dot{d}_i$ ,  $\mathbf{g}_i := \mathbf{g}_i^a$ ,

$\mathbf{g}_{N+i} = \mathbf{g}_i^b = \mathbf{0}$ ,  $\mathbf{g}_{2N+i} := \mathbf{g}_i^c$ . Moreover, we define  $\mathbf{A}$  to be the following block matrix

$$\mathbf{A} := \begin{pmatrix} \mathbf{CK} & -\frac{\text{Ra}}{\delta} \mathbf{C} \mathbf{X}^T & \mathbf{0} \\ \mathbf{0} & \mathbf{0} & \mathbf{I} \\ \delta \mathbf{B}^T \mathbf{CK} + \frac{\delta \mathbf{B}^T}{\text{Sg}} & -\text{Ra} \mathbf{B}^T \mathbf{C} \mathbf{X}^T - \frac{\mathbf{\Pi}_2}{\text{Sg Pr}} & -\frac{\mathbf{I}}{\text{Sg}} \end{pmatrix}, \quad (23)$$

where  $\mathbf{I} := \{\delta_{ij}\}$  is the  $N \times N$  identity matrix,  $\delta_{ij}$  is Kronecker’s delta—not to be confused with the parameter  $\delta$ , and  $\mathbf{0}$  is the zero matrix.

Note that for the Fourier case, we have a  $2N \times 2N$  system and

$$\mathbf{A} = \begin{pmatrix} \mathbf{CK} & -\frac{\text{Ra}}{\delta} \mathbf{C} \mathbf{X}^T \\ \delta \mathbf{B}^T & -\frac{1}{\text{Pr}} \mathbf{\Pi}_2 \end{pmatrix}. \quad (24)$$

With the help of the above notation, we re-write Eqs. (21) in the form  $\dot{\mathbf{y}} = \mathbf{A} \mathbf{y} + \mathbf{g}$ . For the MC case, we obtain a  $3N \times 3N$  system and  $\mathbf{A}$  has  $3N$  eigenvalues, while for the Fourier case,  $\text{Sg} := \mathbf{0}$ , and we have to deal with  $2N$  eigenvalues. This is also the case for  $\text{Sg} \rightarrow \infty$ , but for a different reason: Eq. (8b) can be integrated once in time, reducing thus the overall order of the system.

To simplify our analysis, we define the auxiliary variable  $\Phi(x, t) := \Psi_t(x, t)$ , which when introduced into Eq. (11) yields

$$\Phi_{tx^4} - \Phi_{t^2 x^2} - \text{Ra} \Phi_{xx} = \mathbf{0}. \quad (25)$$

The spectral expansion of  $\Phi$  is obtained from the first expression in Eq. (20), where  $\phi_i := \dot{p}_i$ . Consequently, the corresponding Galerkin system is

$$\kappa_j^4 \dot{\phi}_j - \sum_{i=1}^N \beta_{ij} \ddot{\phi}_i - \text{Ra} \sum_{i=1}^N \beta_{ij} \phi_i = \mathbf{0}. \quad (26)$$

Following the same idea, we formulate a dynamical system in the form  $\dot{\mathbf{y}} = \mathbf{A} \mathbf{y}$ , where  $\mathbf{y}$  is the composite vector of unknowns  $y_i := \phi_i$ ,  $y_{N+i} := \dot{\phi}_i$ ; and now the block matrix of coefficients reads:

$$\mathbf{A} := \begin{pmatrix} \mathbf{0} & \mathbf{I} \\ -\text{Ra} \mathbf{I} & \mathbf{CK} \end{pmatrix}. \quad (27)$$

### 7. Truncated Galerkin series for the eigenvalues

In order to elucidate the approach of this section we begin with a particular set of values for the parameters, namely,

$$\text{Pr} = 0.73, \quad \text{Ra} = 5.0 \times 10^3, \quad \delta = 0.16, \quad (28)$$

and vary the Straughan number. Note that  $\text{Pr} = 0.73$  is a typical value for gases. As is well known, in slow flows, even gases can be regarded as incompressible. We have chosen a large Rayleigh number (the symbol  $\text{Ra}$  in Eq. (28)) here because in the case of  $g$ -jitter, a parametric instability occurs for very large  $\text{Ra}$ . Since thermal relaxation can make the motion more oscillatory, one may generally expect to find instability only when  $\text{Ra}$  is very large. The specific values in Eq. (28) are chosen in order to compare our present findings with our previous works on two-gradient convection [14,16].

In order to check the robustness of the eigenvalue computations and the role of truncation, we solve the eigenvalue problem for different values of  $N$ . We ran several numerical experiments (not presented here) in order to determine the sensitivity of the results to the truncation of the spectral series. Using the software package MATHEMATICA<sup>®</sup>, eigenvalues were obtained for  $N = 1, 3, 7, 15$ ; they are presented in Table 1 for three different Straughan numbers and for the simple Fourier case ( $\text{Sg} := \mathbf{0}$ ), as well as for the limiting case  $\text{Sg} \rightarrow \infty$ .

<sup>2</sup> Even a twenty-term expansion gives accuracy of order  $10^{-7}$ , which makes the proposed method very well suited for the treatment of convective problems in plane-parallel enclosures.

**Table 1**  
Eigenvalues for different number of terms for  $Ra = 5 \times 10^5$ .

$Sg \rightarrow \infty$	$Sg = 1.0$	$Sg = 0.1$	$Sg = 0.01$	$Sg := 0$
<b>Single-term expansion</b>				
$-5.09 \pm 707.09 i$	$-5.09 \pm 680.62 i$	$-5.09 \pm 680.71 i$	$-5.21 \pm 681.58 i$	$-11.85 \pm 680.63 i$
-	-1.00	-10.00	-99.74	-
<b>Three-terms expansion</b>				
$-4.93 \pm 707.09 i$	$-5.62 \pm 706.50 i$	$-5.63 \pm 706.60 i$	$-5.85 \pm 707.50 i$	$-12.54 \pm 705.87 i$
$-19.86 \pm 706.83 i$	$-23.02 \pm 704.62 i$	$-23.04 \pm 705.01 i$	$-23.80 \pm 708.90 i$	$-51.73 \pm 701.36 i$
$-46.48 \pm 705.58 i$	$-42.62 \pm 642.60 i$	$-42.47 \pm 643.39 i$	$-42.16 \pm 651.25 i$	$-101.65 \pm 648.13 i$
-	-1.03	-10.00	-99.34	-
-	-1.00	-10.03	-99.76	-
-	-1.00	-10.24	-99.81	-
<b>Seven-terms expansion</b>				
$-4.93 \pm 707.09 i$	$-5.00 \pm 706.93 i$	$-5.01 \pm 707.02 i$	$-5.14 \pm 707.86 i$	$-11.74 \pm 706.90 i$
$-19.74 \pm 706.83 i$	$-20.04 \pm 706.20 i$	$-20.03 \pm 706.55 i$	$-20.42 \pm 709.93 i$	$-46.95 \pm 706.23 i$
$-44.44 \pm 705.71 i$	$-45.13 \pm 704.27 i$	$-45.06 \pm 705.05 i$	$-45.44 \pm 712.75 i$	$-105.72 \pm 704.91 i$
$-79.10 \pm 702.67 i$	$-80.44 \pm 699.98 i$	$-80.18 \pm 701.36 i$	$-79.59 \pm 715.25 i$	$-188.22 \pm 702.56 i$
$-123.93 \pm 696.16 i$	$-126.45 \pm 691.53 i$	$-125.76 \pm 693.65 i$	$-122.26 \pm 715.68 i$	$-295.04 \pm 698.20 i$
$-179.61 \pm 683.91 i$	$-184.98 \pm 675.78 i$	$-183.46 \pm 678.77 i$	$-173.46 \pm 711.29 i$	$-428.61 \pm 688.50 i$
$-252.43 \pm 660.51 i$	$-241.41 \pm 566.55 i$	$-237.48 \pm 570.01 i$	$-206.35 \pm 613.88 i$	$-574.33 \pm 626.68 i$
-	-1.00	-10.00	-99.36	-
-	-1.00	-10.03	-99.73	-
-	-1.02	-10.19	-99.76	-
-	-1.07	-10.65	-102.47	-
-	-1.17	-11.64	-109.83	-
-	-1.36	-13.54	-125.26	-
-	-1.85	-18.41	-166.64	-
<b>Fifteen-terms expansion</b>				
$-4.93 \pm 707.09 i$	$-4.94 \pm 707.08 i$	$-4.94 \pm 707.16 i$	$-5.06 \pm 708.00 i$	$-11.70 \pm 707.08 i$
$-19.74 \pm 706.83 i$	$-19.75 \pm 706.77 i$	$-19.74 \pm 707.12 i$	$-20.08 \pm 710.51 i$	$-46.78 \pm 706.97 i$
$-44.41 \pm 705.71 i$	$-44.43 \pm 705.58 i$	$-44.35 \pm 706.35 i$	$-44.59 \pm 714.05 i$	$-105.26 \pm 706.69 i$
$-78.96 \pm 702.68 i$	$-78.98 \pm 702.45 i$	$-78.69 \pm 703.81 i$	$-77.84 \pm 717.58 i$	$-187.13 \pm 706.09 i$
$-123.38 \pm 696.26 i$	$-123.38 \pm 695.88 i$	$-85.95 \pm 160.95 i$	$-118.74 \pm 719.45 i$	$-292.41 \pm 704.98 i$
$-177.70 \pm 684.42 i$	$-177.63 \pm 683.82 i$	$-122.66 \pm 697.95 i$	$-132.93 \pm 560.89 i$	$-421.09 \pm 703.08 i$
$-241.91 \pm 664.44 i$	$-241.75 \pm 663.54 i$	$-150.05 \pm 109.42 i$	$-165.89 \pm 717.32 i$	$-573.20 \pm 700.06 i$
$-316.06 \pm 632.54 i$	$-315.72 \pm 631.15 i$	$-176.13 \pm 686.66 i$	$-177.52 \pm 553.84 i$	$-748.77 \pm 695.51 i$
$-400.18 \pm 582.97 i$	$-399.59 \pm 580.75 i$	$-238.91 \pm 667.07 i$	$-207.63 \pm 525.87 i$	$-947.85 \pm 688.94 i$
$-494.36 \pm 505.58 i$	$-493.39 \pm 501.77 i$	$-310.82 \pm 635.03 i$	$-217.41 \pm 707.85 i$	$-1170.53 \pm 679.75 i$
$-598.72 \pm 376.22 i$	$-597.25 \pm 368.48 i$	$-391.57 \pm 584.08 i$	$-248.39 \pm 507.32 i$	$-1416.97 \pm 667.15 i$
		$-480.75 \pm 502.34 i$	$-270.19 \pm 686.40 i$	$-1687.48 \pm 650.08 i$
		$-577.62 \pm 359.00 i$	$-306.27 \pm 515.35 i$	$-1982.85 \pm 626.81 i$
			$-317.78 \pm 646.30 i$	$-2305.84 \pm 593.04 i$
			$-342.23 \pm 580.48 i$	$-2667.60 \pm 497.69 i$
-242.52	-1.00	-10.00	-99.36	-
-302.44	-1.00	-10.03	-99.74	-
-387.21	-1.02	-10.19	-99.76	-
-618.24	-1.07	-10.64	-102.43	-
-808.75	-1.17	-11.60	-109.58	-
-1291.30	-1.35	-13.37	-123.97	-
-1653.20	-1.64	-16.31	-149.43	-
-2061.72	-2.10	-20.91	-192.18	-
	-2.77	-27.80	-265.20	-
	-3.71	-37.97	-404.51	-
	-5.00	-53.20	-684.80	-
	-6.73	-77.83	-1029.48	-
	-9.05	-135.81	-1361.48	-
	-12.23	-245.13	-1697.28	-
	-23.96	-478.98	-2141.78	-
	-139.03	-881.59		
	-282.44	-1309.73		
	-369.46	-1669.76		
	-577.77	-2130.88		
	-845.04			
	-1303.44			
	-1666.74			
	-2129.75			

The conclusion from the results presented in the Table 1 is that (in agreement with the theoretical fifth order of the spectral method) the convergence is very good in the sense that the eigenvalues with lower indexes do not change very much when more terms are taken in the expansion. Even a one-term expansion

is, qualitatively, quite good in predicting the behavior of the system. We mention that the first seven eigenvalues change by less than 1% when increasing the truncation limit from  $N = 15$  to  $N = 20$ . For this reason we do not “overload” the presentation with the values obtained for  $N = 20$ ; we just mention that  $N = 15$

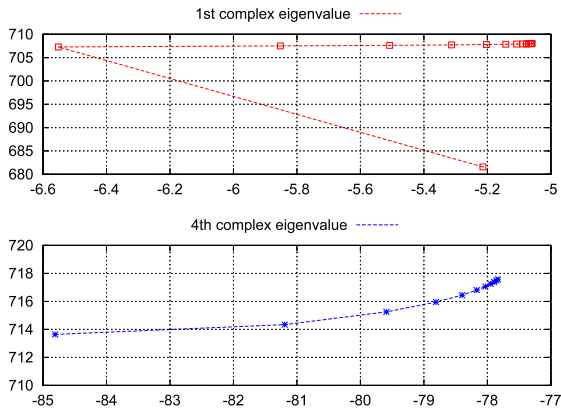


Fig. 4. Convergence of selected eigenvalues with the number of terms  $N$ . Here:  $Sg = 0.01$ ,  $Ra = 5 \times 10^5$ ,  $Pr = 0.73$ ,  $\delta = 0.16$ .

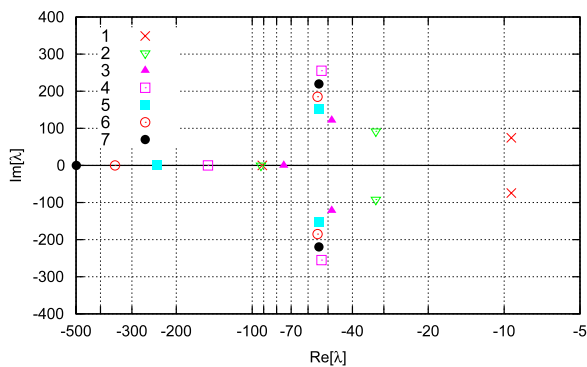


Fig. 5. The distribution of the first several eigenvalues for  $Sg = 0.01$ ,  $Ra = 5 \times 10^5$ ,  $Pr = 0.73$ ,  $\delta = 0.16$ .

turned out to give excellent approximations for the eigenvalues in all the cases presented here. Note also that we have numbered the eigenvalues so that the real parts of those with higher indexes have larger absolute values (i.e., more negative).

### 8. Results and discussion

From Table 1, one sees that the non-oscillatory eigenvalues are all negative and the real parts of the oscillatory modes are also negative, i.e. no growing modes exist. This means that MC-based two-gradient convection is stable for the presented values of  $Sg$ . The first column gives a very good validation of the algorithm because it is computed for a different system, Eq. (26), wherein  $Sg \rightarrow \infty$ , and the comparison with the second column is quantitatively very good for the common eigenfunctions. Note that Eq. (11) has merely  $2N$  eigenvalues (like the case  $Sg := 0$ ), while the full MC model has  $3N$  eigenvalues.

The oscillatory modes, however, change dramatically with the addition of relaxation. As it can be seen in Table 1, the lowest oscillatory eigenvalues have real parts that are less negative than the respective eigenvalues for the pure Fourier case, as presented in the fifth column of Table 1. For a better appreciation of the behavior of the eigenvalues, we have, in Fig. 4, presented results for eigenvalues with index one and four.

For each eigenvalue presented, we begin with the respective numbers of terms in the expansion and increase them further to track how sensitive the results are to truncation; and it is clear that there is a convergence of the respective eigenvalue.

In Fig. 5 we show the distribution of the first seven purely real eigenvalues, and the first seven complex eigenvalues.

One sees that, with the increase of the index, the complex eigenvalues reach a (negative) limit for the real part, i.e., the

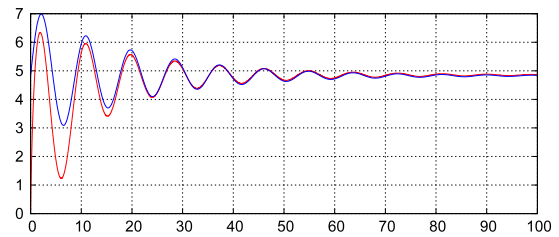


Fig. 6. Time evolution of the stream function at the point  $x = 0.9$  for  $Ra = 5000$ ,  $Pr = 0.73$ ,  $Sg = 0.1$ . The numerical solution (red/solid line) compared to a properly scaled function as given by the lowest eigenmode  $\mu = -4.93652 - 71.4876i$  (blue/dashed line).

ability of the system to damp the oscillatory motion saturates to approximately  $-100$  for  $Sg = 0.01$ . This defines a clear time scale for the decay of the oscillatory motion connected with the inverse of the limit of the real part of the eigenvalues. This is not the case, however, for the Fourier model, where the real parts of the eigenvalue continue decreasing with the eigenvalue index.

One can clearly see the two-pronged effect of including thermal relaxation. First, relaxation gives rise to real, purely negative, eigenvalues which act to speed up, relative to Fourier's law, the dissipation of energy distributed over these modes. Second, the energy partitioned over the oscillatory modes decays more slowly, and the oscillations are somewhat faster (the imaginary parts can be twice as big as the respective imaginary parts of the Fourier case). This means that the oscillatory transients will decay in a longer time, making the system less damped, as far as oscillations are concerned. This might have the effect of lowering the threshold of instability; however, a conclusive answer to this important question must await the results of future investigations of two-dimensional flows.

These observations are fully aligned with the prediction from the general estimates done above.

On a more quantitative basis, we sought to verify our results by means of direct numerical integration of System (21). We began with the trivial initial condition  $p_i(0) = 0$ ,  $d_i(0) = \dot{d}_i(0) = 0$ ,  $i = 1, 2, \dots, N$ , and integrated until the stationary solution from Eqs. (19) was reached. The results we obtained compared with Eqs. (19) within a couple of percentage points over the entire interval  $x \in [-1, 1]$ . Naturally, this happens only when a stable evolution takes place, and the motion itself is oscillatory because of the presence of the modes with nontrivial imaginary parts. A similar case for  $Ra = 5 \times 10^5$  is seen in Table 1. For  $Sg \leq 0.1$ , the real part of the lowest oscillatory mode is less negative than the lowest non-oscillatory mode. This means that for reasonably small  $Sg$ , the non-oscillatory transient in the solution dies out quickly, and the oscillatory one remains and is observed in the direct numerical integration of Eqs. (19). Fig. 6 shows this effect.

Lastly, we carried out one more verification: we determined the onset of instability for the direct numerical solution. We found that it occurs for the same values of the governing parameters for eigenmodes with positive real parts exist. Naturally, the time increment was chosen sufficiently small in order to avoid numerical instability.

### 9. Invariance issues

In [22], it was pointed out that Eq. (1) leads to a paradox in the case of thermal shock propagation, but that the physically unrealistic behavior observed could be eliminated if the convective time derivative was used *in lieu* of  $\partial_t$  in the MC law. The resulting 'convective' MC law<sup>3</sup> is given by

<sup>3</sup> An interesting development of Eq. (29) in the thermodynamical framework is outlined in a recent article by Ostoja-Starzewski [23].

$$\mathbf{q} + \tau_0(\partial_t + \mathbf{v} \cdot \nabla)\mathbf{q} = -K\nabla T, \quad (29)$$

which we observe is Galilean invariant, thus resolving the aforementioned paradox. It should be noted that the system consisting of Eqs. (2), (29) is valid for any kind of material continuum; one has only to close the system by including the appropriate forms of the continuity and momentum equations, as well as constitutive relation(s) for the stress.

Unfortunately, in more than one-dimension, the ‘convective’ MC law of [22] is inextricably coupled to Eq. (2), because the heat flux  $\mathbf{q}$  cannot be eliminated between the two equations. This suggested that a further refinement of the MC law might be possible; and it would be based on an even more general invariant temporal rate operator. It should be noted here that other researchers have investigated the possibility of formulating a frame-indifferent generalization of the MC law. In 1969, Fox [24] proposed a generalization of the MC law based on the Jaumann invariant time derivative. In 1984, Franchi and Straughan [6] investigated the implications of Fox’s re-formulation in the setting of Bénard convection. The situation became somewhat ambiguous when in [7], it was shown that the model based on the Jaumann rate predicts a direction for the convective vortices that is opposite of the expected one.

Recently, it was argued in [25] that a different frame indifferent objective rate should be used in the MC law, namely, the upper-convected Oldroyd derivative, which results in

$$\tau_0[\partial_t \mathbf{q} + \mathbf{v} \cdot \nabla \mathbf{q} - \mathbf{q} \cdot \nabla \mathbf{v} + (\nabla \cdot \mathbf{v})\mathbf{q}] + \mathbf{q} = -K\nabla T. \quad (30)$$

One of the main advantages of using the last equation is that it leads to a single equation for the temperature field. Following the gist of a similar derivation for the displacement current given in [26], it is also shown in [25] that the flux vector  $\mathbf{q}$  can be eliminated between Eqs. (2) and (30), thus yielding

$$\tau_0[T_{tt} + 2\mathbf{v} \cdot \nabla T_t + \mathbf{v}_t \cdot \nabla T + (T_t + \mathbf{v} \cdot \nabla T)(\nabla \cdot \mathbf{v}) + \mathbf{v} \cdot \nabla(\mathbf{v} \cdot \nabla T)] + T_t + \mathbf{v} \cdot \nabla T = \kappa \nabla^2 T, \quad (31)$$

a single equation for the temperature field, just as in the case of (the much simpler) Eq. (3).

At this juncture, it is important to investigate what are the effects related to frame-indifference that are not present in Eq. (1). In the case of thermo-compressible flow, the investigation of this issue has already begun; see [27], wherein the propagation of acoustic waves and second-sound in fluids are studied. Simultaneously, the mathematical issues connected with the new model have also received attention [28]. It is important to understand that, in an incompressible flow of the type of the considered here, two-gradient convection can provide an opportunity to investigate the role of the different terms in the invariant time rate of the flux.

In order to identify the role of the different components of the heat flux, we return to the equations for the energy conservation, Eq. (2), heat flux Eq. (29), and the momentum equations, Eq. (4), and consider them in 1D. Below, so as to distinguish from the vector quantities, we use capital letters for the dependent variables, and the aforementioned equations reduce to the following system:

$$\frac{\partial V}{\partial t} = -\frac{Ra}{\delta} \left[ \Theta(x, t) + \frac{x}{2} \right] + \frac{\partial^2 V}{\partial x^2}, \quad (32a)$$

$$Sg \frac{\partial Q}{\partial t} + Q(x, t) = -\frac{\partial \Theta}{\partial x}, \quad (32b)$$

$$Sg \frac{\partial R}{\partial t} - Q(x, t) \frac{\partial V}{\partial x} = -Pr R(x, t), \quad (32c)$$

$$\frac{\partial \Theta}{\partial t} + \delta V(x, t) = -\frac{\partial Q}{\partial x}. \quad (32d)$$

Here,  $Q$  and  $R$  denote the dimensionless horizontal and vertical components of the heat flux, respectively. Eq. (32a) presents the momentum equation for the vertical component from Eqs. (4). (The other two momentum equations are trivial because there are no horizontal and transversal components of the velocity.) Eqs. (32d) and (32b) are for the temperature and the horizontal component of the heat flux, respectively.

We mention here that the equation for the vertical component of the flux, Eq. (32c), splits out from the rest of the system, i.e. the terms connected with the convective derivative of the heat flux vanish identically in the other equations. Yet, System (32) shows that the vertical component of the flux,  $R$ , can be found after the other three equations are solved; i.e., two-gradient convection flows can play an important role in assessing the applicability of frame-indifferent models, provided that measurements of the vertical component of the heat flux, *not based* on Fourier’s law, are available. Specifically, the heat flux must be measured directly, without inferring it from the temperature and/or its gradient.

## 10. Conclusions

We considered the convective flow of a thermo-viscous fluid in a vertical slot, subject to both vertical and horizontal temperature gradients, as a model system for investigating the role played by thermal relaxation, as it occurs in the Maxwell–Cattaneo (MC) law. Our main conclusion is that the MC law enhances the oscillatory character of the motion, despite the fact that under certain circumstances (i.e., certain velocity and temperature profiles) relaxation can also play a dissipative role. The convection was found to be stable for all values of the Straughan number considered, albeit more oscillatory than the Fourier case. The properties of MC-based convection revealed here can have a profound impact on unsteady convective flow, as in the case of so-called *g-jitter* flow, where the additional oscillations introduced by the presence of relaxation can lead to resonance effects. Our findings can have important consequences for 2D flows as well, where relaxation may lead to qualitative differences from those based on Fourier’s law.

Finally, we also reposed the problem in terms of the frame-indifferent MC model, involving the Oldroyd upper-convected time derivative, given in Eq. (30). We showed that the two-gradient convective flow considered here can be used to elucidate the role of the upper-convected terms, provided that measurements of the heat flux, independent of the temperature and its gradient, are available.

## Acknowledgements

The work of C.I.C. was supported, in part, by an 2009 ASEF/ONR Summer Faculty Fellowship. C.I.C. gratefully acknowledges the hospitality of Dr. Stanley A. Chin-Bing, and the members of his research group, during his stay at the US Naval Research Laboratory, Stennis Space Center, Mississippi, USA. P.M.J. was supported by ONR/NRL funding (PE 061153N).

The authors thank the two anonymous referees, and Prof. Frédéric Dias, for their helpful comments and instructive suggestions. The authors also thank Dr. Douglas Todoroff for pointing out a number misprints and omissions in an earlier draft of this work.

## Appendix. Properties of beam functions

Beam functions are defined as

$$s_m = \frac{1}{\sqrt{2}} \left[ \frac{\sinh \lambda_m x}{\sinh \lambda_m} - \frac{\sin \lambda_m x}{\sin \lambda_m} \right], \quad \coth \lambda_m - \cot \lambda_m = 0,$$

$$c_m = \frac{1}{\sqrt{2}} \left[ \frac{\cosh \kappa_m x}{\cosh \kappa_m} - \frac{\cos \kappa_m x}{\cos \kappa_m} \right], \quad \tanh \kappa_m + \tan \kappa_m = 0.$$

They are the eigenfunctions of the fourth-order Sturm–Liouville b.v.p.

$$\frac{d^4 u}{dx^4} = \lambda^4 u, \quad u = \frac{du}{dx} = 0, \quad \text{for } x = \pm 1.$$

The relevant derivatives of the beam functions are

$$c'_n = \sum_{m=1}^{\infty} a_{nm} s_m, \quad s'_n = \sum_{m=1}^{\infty} \bar{a}_{nm} c_m,$$

$$c''_n = \sum_{m=1}^{\infty} \beta_{nm} c_m, \quad s''_n = \sum_{m=1}^{\infty} \bar{\beta}_{nm} s_m,$$

where

$$a_{nm} = -\bar{a}_{mn} = \frac{4\kappa_n^2 \lambda_m^2}{\kappa_n^4 - \lambda_m^4},$$

$$\beta_{mm} = \begin{cases} \frac{4\kappa_n^2 \kappa_m^2}{\kappa_m^4 - \kappa_n^4} (\kappa_m \tanh \kappa_m - \kappa_n \tanh \kappa_n), & m \neq n, \\ \kappa_n \tanh \kappa_n - (\kappa_n \tanh \kappa_n)^2, & m = n, \end{cases}$$

$$\bar{\beta}_{mm} = \begin{cases} \frac{4\lambda_n^2 \lambda_m^2}{\lambda_n^4 - \lambda_m^4} (\lambda_n \coth \lambda_n - \lambda_m \coth \lambda_m), & m \neq n, \\ \lambda_n \coth \lambda_n - (\lambda_n \coth \lambda_n)^2, & m = n. \end{cases}$$

The expansion of unity reads

$$1 = \sum_{k=1}^{\infty} h_k c_k(x), \quad h_k = \int_{-1}^1 c_k(x) dx = \frac{2\sqrt{2} \tanh \kappa_k}{\kappa_k}.$$

The cross expansions between the harmonic functions and the beam functions are given by

$$\sin l\pi x = \sum_{k=1}^{\infty} \sigma_{lk} s_k(x), \quad \sigma_{lk} = \frac{2\sqrt{2}l\pi (\lambda_k)^2 (-1)^l}{l^4 \pi^4 - \lambda_k^4},$$

$$\cos l\pi x = \sum_{k=1}^{\infty} \chi_{lk} c_k(x), \quad \chi_{lk} = \frac{2\sqrt{2}\kappa_k^3 (-1)^{l+1} \tanh \kappa_k}{l^4 \pi^4 - \kappa_k^4},$$

$$c_n(x) = \sum_{l=1}^{\infty} \hat{\chi}_{nl} \cos l\pi x, \quad \hat{\chi}_{nl} = \frac{2\sqrt{2}\kappa_n^3 (-1)^{l+1} \tanh \kappa_n}{l^4 \pi^4 - \kappa_n^4},$$

$$s_n(x) = \sum_{l=1}^{\infty} \hat{\sigma}_{nl} \sin l\pi x, \quad \hat{\sigma}_{nl} = \frac{2\sqrt{2}l\pi (\lambda_n)^2 (-1)^l}{l^4 \pi^4 - \lambda_n^4}.$$

## References

[1] P.M. Jordan, W. Dai, R.E. Mickens, A note on the delayed heat equation: instability with respect to initial data, *Mech. Res. Comm.* 35 (2008) 414–420.  
 [2] D.D. Joseph, L. Preziosi, Heat waves, *Rev. Modern Phys.* 61 (1989) 41–73.

[3] D.D. Joseph, L. Preziosi, Addendum to the paper "Heat waves", *Rev. Modern Phys.* 61 (1989) 41; *Rev. Modern Phys.* 62 (1990) 375–391.  
 [4] D.S. Chandrasekharaiah, Hyperbolic thermoelasticity: a review of recent literature, *Appl. Mech. Rev.* 51 (1998) 705–729.  
 [5] D. Jou, J. Casas-Vázquez, G. Lebon, Extended irreversible thermodynamics revisited (1988–98), *Rep. Progr. Phys.* 62 (1998) 1035–1142.  
 [6] B. Straughan, F. Franchi, Bénard convection and the Cattaneo law for heat conduction, *Proc. Roy. Soc. Edinburgh Sect. A* 96 (1984) 175–178.  
 [7] G. Lebon, A. Clout, Bénard–Marangoni instability in Maxwell–Cattaneo fluids, *Phys. Lett. A* 105 (1984) 361–364.  
 [8] B. Straughan, Thermal convection with the Cattaneo–Christov model, *Int. J. Heat Mass Transfer* 53 (2010) 95–98.  
 [9] J.W. Elder, Laminar free convection in a vertical slot, *J. Fluid Mech.* 23 (1965) 77–98.  
 [10] A. Farooq, G.M. Homsy, Streaming flows due to g-jitter-induced natural convection, *J. Fluid Mech.* 271 (1994) 351–378.  
 [11] A. Farooq, G.M. Homsy, Linear and nonlinear dynamics of a differentially heated slot under gravity modulation, *J. Fluid Mech.* 313 (1996) 1–38.  
 [12] P.S. Grassia, G.M. Homsy, Buoyant flows with low-frequency jitter, *Phys. Fluids* 10 (1998) 1903–1923.  
 [13] S.A. Vinod, C.I. Christov, G.M. Homsy, Resonant thermocapillary and buoyant flows with finite frequency gravity modulation, *Phys. Fluids* 11 (1999) 2565–2576.  
 [14] C.I. Christov, G.M. Homsy, Nonlinear dynamics of two dimensional convection in a vertically stratified slot with and without gravity modulation, *J. Fluid Mech.* 430 (2001) 335–360.  
 [15] X.H. Tang, C.I. Christov, Nonlinear waves of the steady natural convection in a vertical fluid layer: a numerical approach, *Math. Comput. Simulation* 74 (2007) 203–213.  
 [16] N.C. Papanicolaou, C.I. Christov, G.M. Homsy, Galerkin technique based on beam functions in application to the parametric instability of thermal convection in a vertical slot, *Internat. J. Numer. Methods Fluids* 59 (2009) 945–965.  
 [17] C.I. Christov, Frame indifferent form of Maxwell–Cattaneo law, in: M. Ostoja-Starzewski, P. Marzocca (Eds.), *Proceedings of the 8th International Congress on Thermal Stresses*, TS2009, vol. II, UI, 2009, pp. 543–546.  
 [18] P.M. Jordan, Growth, decay and bifurcation of shock amplitudes under the type-II flux law, *Proc. R. Soc. A* 463 (2007) 2783–2798.  
 [19] S. Chandrasekhar, *Hydrodynamic and Hydromagnetic Stability*, Oxford University Press, Clarendon, London, 1961.  
 [20] C.I. Christov, A method for treating the stochastic bifurcation of plane Poiseuille flow, *Ann. Univ. Sof., Fac. Math. Mech.* 76 (1982) 87–113.  
 [21] N.C. Papanicolaou, C.I. Christov, On the beam functions spectral expansions for fourth-order boundary value problems, in: *AIP Conf. Proc.*, vol. 946, AIP, 2007, pp. 119–126.  
 [22] C.I. Christov, P.M. Jordan, Heat conduction paradox involving second sound propagation in moving media, *Phys. Rev. Lett.* 94 (2005) 154301.  
 [23] M. Ostoja-Starzewski, A derivation of the Maxwell–Cattaneo equation from the free energy and dissipation potentials, *Internat. J. Engrg. Sci.* 47 (2009) 807–810.  
 [24] N. Fox, Generalised thermoelasticity, *Internat. J. Engrg. Sci.* 7 (1969) 437–445.  
 [25] C.I. Christov, On frame indifferent formulation of the Maxwell–Cattaneo model of finite-speed heat conduction, *Mech. Res. Comm.* 36 (2009) 481–486.  
 [26] C.I. Christov, On the material invariant formulation of Maxwell's displacement current, *Found. Phys.* 36 (2006) 1701–1717.  
 [27] B. Straughan, Acoustic waves in a Cattaneo–Christov gas, *Phys. Lett. A* 374 (2010) 2556–2667.  
 [28] M. Ciarletta, B. Straughan, Uniqueness and structural stability for the Cattaneo–Christov equations, *Mech. Res. Comm.* 37 (2010) 445–447.